ISSN: 0369-8963

Segmentation of Mammogram Abnormalities Using Ant System Based Contour Clustering Algorithm

1*SUDHA. S, 2GANESAN. R

1Department of Master of Computer Applications, RVS College of Engineering,

Dindigul - 624005, Tamil Nadu, India.

2Department of Electrical and Electronics Engineering, E.G.S. Pillay Engineering College,

Nagapattinam - 611002, Tamil Nadu, India.

ABSTRACT

Background: The Computer-Aided Detection Systems (CADs) can locate and identify the normal and pathological tissues in mammogram images by segmentation. The existing segmentation methods have to test each and every pixel of the image at least once, which is computationally expensive.

Objective: This research focuses on detection of microcalcifications from the digital mammograms by segmentation, where the abnormal tissues are segmented from the normal tissues.

Methods: To detect microcalcifications from the digital mammograms by segmentation, a novel segmentation approach based on Ant Clustering method namely Ant System based Contour Clustering (ASCC), simulates the ants' foraging behavior is proposed. The proposed ASCC is compared with the state-of art existing methods with respect to area, pixel and edge based metrics on the Mammographic Image Analysis Society (MIAS) Dataset.

Results: The segmentation performance of the proposed ASCC method is experimented on 312 digitized mammogram images acquired from the 161 patient's left and right breast Screening. The segmentation by the proposed ASCC is evaluated by the area, pixel and edge based metrics shows that 62.47% common area between overlapping segmented and the reference region by Jaccard index, Goodness based on inter-region contrast of 66.59%, Low Segmentation Error of 9.51%, precision of 93.67%, Recall of 90.90%, 0.85% Figure of Merit, Over-segmented Pixel Rate of 0.43%, and Under-Segmented Pixel Rate of 0.26%.

Conclusion: Segmentation is key preprocessing method to accurately locate and identify the normal and pathological tissues in digital mammogram images. This study proposes an ASCC method for segmentation task by hybridizing clustering and contour based segmentation approaches. The evaluated results with respect to area, pixel and edge based metrics shows added advantage in segmentation tasks compared to the other approaches.

Keywords: *Mammogram Image, Segmentation, Ant System, Ant Colony Optimization, Contour and Clustering*

INTRODUCTION

Breast cancer has the highest incidence rate among women in most countries. Initially it seems to be an asymptomatic breast lesion, and then it may extend to the entire organ if untreated. Breast cancer statistics report says that the incidence rate rises among all other cancers in women worldwide. According to the World Health Organization (WHO), breast cancer will become the most common cancer globally as of 2021, accounting for 12% of all new annual cancer cases worldwide. In India,

 https://doi.org/10.37896/pd91.4/91426

ISSN: 0369-8963

breast cancer is widespread in urban areas and contributes about 25-35% of all cancers in women. Breast cancer starts in milk ducts or the lobules and spreads across the breast tissues. The specific causes of breast cancer are yet to identify. However, some risk factors might be the reason for developing breast cancer. Some of the risk factors are menopause delay, heritage, hormone therapy and dietary factors. Digital Mammography outperforms the other available screening options, such as Computed Tomography (CT), Magnetic Resonance Imaging (MRI) and Ultrasound. The mammographic image consists of non-pathological structures. In these structures, 10% to 25% of the masses are overlooked by the radiographers [1]-[3]. False-negatives are a severe issue in practical screening. The visual tiredness and consistency of the radiologists have increased a great demand for developing CAD system for analyzing mammogram images.

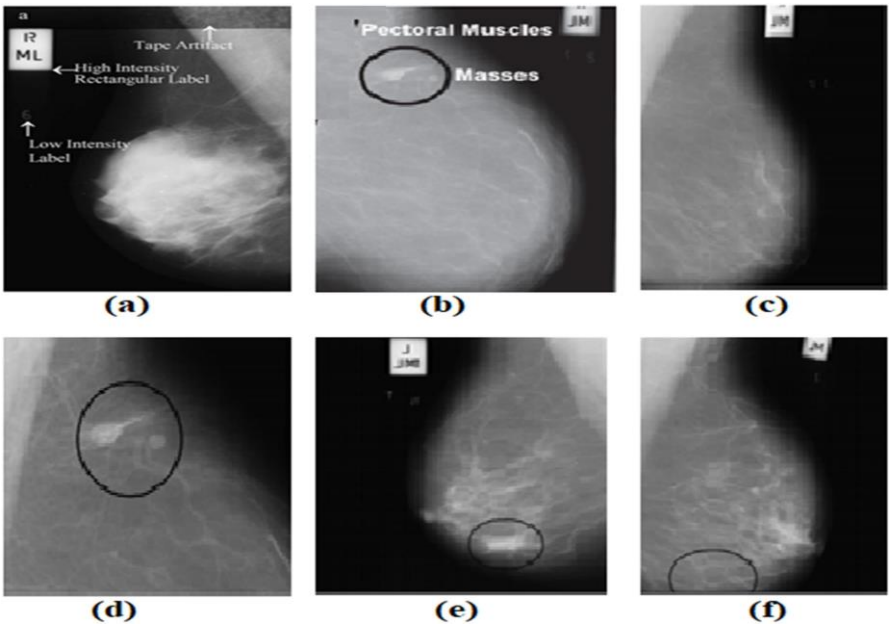

Fig.1. Mammogram samples images (a) Image with noises and artifacts (b) Multi-Lateral Oblique (MLO) View (c) Normal (d) Presence of microcalcifications clusters (e) Left bilateral asymmetry (f) Right bilateral asymmetry

https://doi.org/10.37896/pd91.4/91426

ISSN: 0369-8963

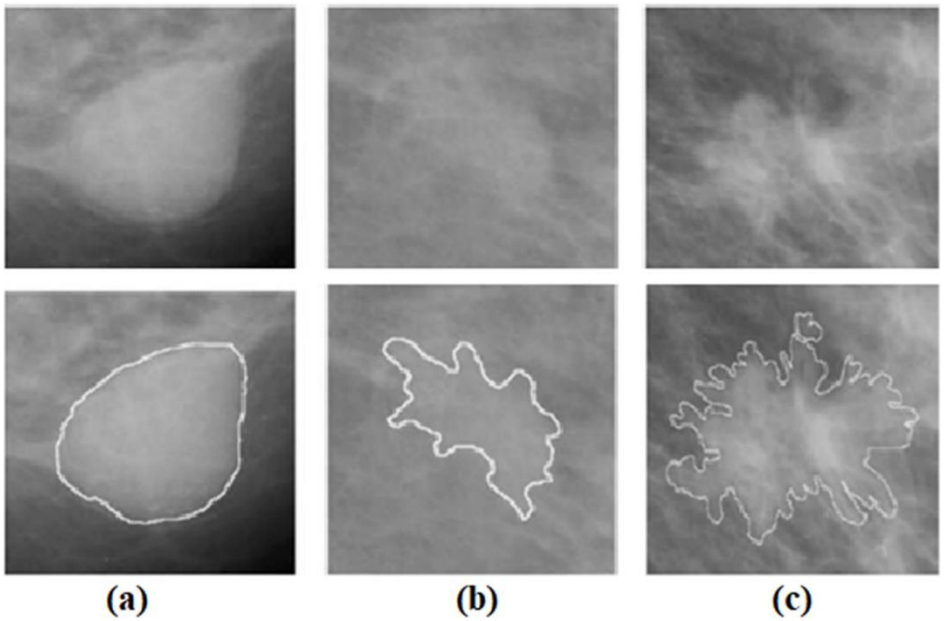

Fig.2. Sample Mammogram Masses (a) circularly shaped (b) defined shape (c) unevenly shaped

The shape and size of the tumors are irregular, which encounters the CAD systems complicated in mammogram analysis. The sample mammogram images are depicted in Fig.1. The Microcalcifications and masses appear as small bright spots. The individual microcalcifications can be of size from 20 to several 100 microns in diameter. Various types of masses, based on their shape, boundary and characterized as circumscribed, well-defined, spiculated, or ill-defined as shown in Fig.2. The radiologists investigate these associated findings to classify them as malignant or benign. In general, benign regions would be round or oval, whereas malignant regions are partially rounded shape with uneven boundaries. The mass detection is more challenging than locating microcalcifications due to size and shape variation and poor contrast [4].

CAD systems can help experts make desired decisions in the analysis [5]. They use automated or partially automated phases to aid in mammogram image analysis [6]. The CAD aims to improve classification and reduce false positives. Sensitivity measures the diagnostic accuracy of CAD systems, while specificity analyses the discrimination accuracy between benign and malignant cases. The healthcare practitioner may consider previously reported cases to decide and diagnose breast cancer. There are numerous methods for performing segmentation of breast mammogram images with Ant based systems to perform Ant Colony Optimization (ACO), and Ant clustering. The segmentation methods such as Fuzzy C-Means (FCM), k-means clustering, Quality Thresholding (QT), Active Contour (AC) based segmentation, and Level Set (LS) segmentation can segment the breast masses with better precision and recall values. However, the major limitation of these methods is that they have to test every pixel of the image at least once, which is computationally expensive. There is no optimal value to initialize the ant system parameters like number of ants, maximum number of iterations and thresholds employed in the similarity functions. Due to these limitations, the existing techniques could not perform well and to help the healthcare practitioner, a novel method required to segment the mammogram images for breast cancer.

 https://doi.org/10.37896/pd91.4/91426

ISSN: 0369-8963

RELATED WORKS

In practice, the diagnosis results may not be similar between the radiologists; hence a second opinion could be made from the automated system to confirm the prognosis results. Therefore, detection of microcalcifications from the digital mammograms by segmentation of the mammogram images, where the abnormal tissues are segmented from the normal tissues is required to develop with new novel techniques by considering the area, pixel and edge metrics in an evaluation. Considering the image segmentation as an optimization problem has a couple of difficulties. The high-resolution images have larger search space, and the non-convex objective function may lead to many local minima. An Ant Colony System (ACS) hybrid with Markov Random Field (MRF) for image segmentation is proposed by Ouadfel et al. [7]. Han et.al [8] proposed an Ant Colony Optimization (ACO) based fuzzy clustering for image segmentation. The fuzzy membership function is estimated based on pixels' gray value, gradient and adjacency. The cluster centers are improved heuristically which enhances the searching process. Abdullah and Jasim [9] applied an ACO for document image segmentation and reported a greater accuracy of 96.95%. Khorram and Yazdi [10] developed an optimized thresholding method for brain image segmentation which used to estimate the optimum threshold, where the texture features are adopted as heuristic information.

Estevez et al. in [11] presented an Interactive Selective and Adaptive Clustering (ISAAC) for locating small sized masses in mammograms. Riyahi-Alam et al. [12] demonstrated a Subtractive Clustering (SC) based mammogram segmentation carried out with 47 mammogram images reported a greater accuracy of 87% and an average of 0.5 false positives per image. Santoro et al. [13] presented a Fuzzy C-Means (FCM) clustering-based mammogram image segmentation by which mammogram images are represented using a local power spectrum with a set of Gabor filters. The segmentation is achieved with FCM clustering. Bhattacharya and Das [14] proposed a FCM-based clustering for mammogram image segmentation where morphological and discrete wavelet transforms are used in preprocessing steps. Boss et al. [15] offered a texture feature-based FCM clustering for mammogram segmentation. The classification results with lower error rate indicate the superior performance of the FCM over k-means clustering. Chowdhary and Acharjya [16] presented a novel intuitionistic PFCM for mass detection. Intuitionistic PFCM is a hybrid method of intuitionistic FCM and Possibilistic FCM.

Rouhi, R. et.al [17] developed a hybrid level set segmentation in which fuzzy clustering and region growing concepts perform mammogram images' segmentation and the classification performance is evaluated with area under the ROC (Receiver Operating Characteristic) curve measure estimated with a Support Vector Machine (SVM) classifier [18]. However, this method provides segmentation with noise and artifacts. Joberth de Nazare Silva et al. [19] proposed a Quality Thresholding (QT) for automatic detection of masses in mammograms using clustering method. Then the appropriate masses are identified with a SVM classifier. The investigation results report a classification rate of 83.53%, demonstrating the significance of the QT based mass segmentation. Liu et al. [20] proposed a muscle segmentation using the Otsu thresholding and the multiple regression method in mammogram images. The method is based on the position localization of pectoral muscles in a breast region by combining the Otsu thresholding method and mathematical morphology.

Sandhya et al. [21] proposed an advanced k-Means clustering method hybrid with the homomorphic filtering for mammographic mass segmentation. The experimental results indicate that the filtering improves the clustering results significantly. A dynamic k-means clustering algorithm based mammogram image segmentation is presented by Elmoufidi et al. [22]. Here, the optimum numbers of clusters are dynamically estimated by Local Binary Pattern (LBP) method. The performance of the

 https://doi.org/10.37896/pd91.4/91426

ISSN: 0369-8963

dynamic k-means clustering based segmentation is analyzed with MIAS database, and reported a lower false positive rate of 2.84. Wan and Zunaidi [23] presented an adaptive k-means clustering for mammogram segmentation and demonstrated the significance with greater accuracy of 94.3% from SVM classifier. Moftah et al. [24] proposed an adaptive k-means method, where the adaptiveness is achieved by refining the cluster centers with the circularity and goodness metrics. The experimental results indicate the superior performance of the adaptive k-means method.

Many studies have been conducted on the segmentation of mammogram images. However, still there are some issues to be solved by developing a segmentation approach which consider all the existing challenges. The existing mammogram databases contain noisy images as they are received from old X-ray films. Hence it requires an additional step to preprocess the images to remove noises. However, the noise removal algorithms might disturb the mass boundaries, and make them hard. These disruptions might degrade the segmentation performance. More efficient preprocessing algorithms are required to address this issue. Another preprocessing step required in MLO view based mammogram image is to remove the pectoral muscle, as they share similar gray-level similar to mass regions. Developing a robust segmentation algorithm that does not require eliminating the pectoral region is necessary. More robust segmentation is expected to reduce the false positive rate, which should not partition the normal tissues as masses. Otherwise the feature values estimated from these regions might be ambiguous and affect the classification performance. The features are generally derived from the regions of interest to classify the masses. However, there is no evidence for an optimal feature set to improve the diagnosis performance. Numerous works has been reported to improve segmentation accuracy. However, it is still expected to explore hybrid intelligence to overcome the drawbacks of the reported segmentation methods. The clustering and contour based methods are integrated in this research work to locate the mammogram abnormalities efficiently.

METHODOLOGY

There may be differences between the radiologists' diagnosis results. Thus an automated system can provide a second opinion. Therefore, the development of new approaches for detecting microcalcifications from digital mammograms via segmentation of the mammography images, where the abnormal tissues are divided from the normal tissues, is essential. A novel segmentation strategy based on the Ant Clustering method, Ant System based Contour Clustering (ASCC) that simulates the ants' foraging behavior, is proposed to detect microcalcifications from digital mammograms by segmentation. This segmentation method provides adequate segmented results to the practitioner to perform the surgical procedure. This study proposes an ASCC method for segmentation task by hybridizing clustering and contour based segmentation approaches. In this work, initially, Ant Clustering model for Image Segmentation is presented in which image pixels are transformed from 2D to 1D array, where each cell can contain only one pixel and the clustering procedure starts when each ant is allowed to choose a pixel at random and back to its nest. Further, we have presented the proposed Ant System based Contour Clustering (ASCC) by which the limitations of the Ant Clustering are overcome. The proposed ASCC is compared with the state-of art existing methods with respect to area, pixel and edge based metrics on the Mammographic Image Analysis Society (MIAS) Dataset.

Ant Clustering Model for Image Segmentation

The baseline ant clustering model discussed by Deneuborug et al. in [25] is to pick up the isolated objects and drop them at another location where more objects of that kind are present. For an illustration, consider only one type of object in the search space. The pick probability p_{pick} to pick up

 https://doi.org/10.37896/pd91.4/91426

ISSN: 0369-8963

an object is computed as

$$p_{pick} = \left(\frac{k_1}{k_1+f}\right)^2 \quad (1)$$

where, f is the perceived fraction of objects adjacent to the ant and k_1 is a threshold factor between 0 and 1.

Similarly, the drop probability $p$drop for a loaded agent to drop the object is defined as

$$p_{drop} = \left(\frac{f}{k_2+f}\right)^2 \quad (2)$$

where, k_2 is another threshold factor between 0 and 1.

Lumer and Faieta [26] extended Deneuborug's [25] ant clustering model. Here the similarity between the objects is estimated by using a neighborhood location, defined as

$$f(i) = max\left(0, \frac{1}{\sigma^2}\sum_j \left(1 - \frac{\delta(i,j)}{\alpha}\right)\right) \quad (3)$$

where α is a threshold factor for the distance metric $\delta(i,j)$ between a picked object i and all the adjacent objects j. It is suggested to restrict the neighborhood size as either 3×3 or 5×5. The pick and drop probabilities are defined based on neighborhood function with the below equations:

$$p_{pick}(i) = \left(\frac{k_1}{k_1+f(i)}\right)^2 \quad (4)$$

and

$$p_{drop}(i) = \begin{cases} 2f(i), & if\ f(i) < k_2 \\ 1, & otherwise \end{cases} \quad (5)$$

Where, k_1 and k_2 parameters are used to represent the amount of influence over the f has over pick up and drop probabilities. For an object i when its similarity value is low with respect to k_1, then an unloaded ant is likely to pick up that object. Similarly, when the similarity value is high with respect to k_2, represents that the agent reaches the location where it finds more similar objects. Hence it is likely to drop the carrying objects. Subsequently, this procedure constructs the clusters in 2D space. Each ant has a heap to store a list of recently visited objects in the ant clustering model. With that list, when an ant picks up an object, it can compare with the recently visited objects and choose to move towards the most similar item from the list. This process is known as Matching Search. In the basic ant clustering algorithms, the ants can walk around on a two-dimensional grid, where the grid size is fixed based on the input size. It is difficult for the ants to find a location to drop the object with the smaller grid size. In the other case, if the grid size is too huge, then the ants will be idle for a long time to pick up an object. Hence, the grid size should be optimum enough to avoid such time complexity.

In the AntClust algorithm, initially the image pixels are transformed from 2D to a 1D array, where each cell can contain only one pixel. At the first step, from *K* number of ants, each ant is allowed to choose a pixel at random and back to its nest. Then the clustering procedure starts. At this time the ants are allowed to move between their nest and the cells of the array. While visiting a cell, the ant can decide whether or not to drop the pixel to the current cell based on the probability, p_{drop}. Suppose, an ant drops the pixel, then the ant is free now, and it starts searching for the other pixel to pick up from the list of unvisited or unloaded pixels. This iterative process could be terminated by fixing the maximum number of iterations.

The similarity function f, for picking or dropping is pixel p_i from a cell c_k is defined as

$$f(p_i, c_k) = \frac{1}{n_k}\sum_{p_j \in c_k} \frac{\alpha^2}{\alpha^2 + \delta(p_i,p_j)^2} \quad (6)$$

where $\delta(p_i, p_j)$ represents the distance measure, which estimates the gray level intensity variation

 https://doi.org/10.37896/pd91.4/91426

ISSN: 0369-8963

between p_i and p_j pixels as

$$\delta(p_i, p_j) = \frac{|g_i - g_j|}{NG} \tag{7}$$

where g_i and g_j represents the intensity value of the pixels p_i and p_j respectively, and NG denotes the maximum intensity value of the image. The symbol α indicates the average distance between all pixels and is given as

$$\alpha = \frac{1}{N(N-1)} \sum_{i=1}^{N} \sum_{j=1}^{N} \delta(p_i, p_j) \tag{8}$$

This could be estimated prior to the clustering procedure. The similarity function f returns a maximum value when the distance is zero. The pickup and dropping procedure for the Ant Clustering algorithm is explained below:

Picking up a pixel

When the ant is unloaded, it searches for a free pixel based on an index table which consists of all unloaded pixels. For an unloaded ant, the following three situations are considered to pick up a pixel

- A cell contains only one pixel, then the ant picks it.
- A cell that contains two dissimilar pixels, then the ant destroys this cluster and picks up a pixel based on probability q, a random number between 0 and 1.
- In a cell of more pixels, where an isolated pixel is found with lower similarity to all other pixels, then the ant chooses that pixel.

These three cases are mathematically represented as pick probability,

$$p_{pick}(p_i, c_k) = \begin{cases} 1 & if\ |c_k| = 1 \\ q & if\ |c_k| = 2 \\ cos^2\left(\frac{\pi}{2} f(p_i, c_k\right) & otherwise \end{cases} \tag{9}$$

Dropping a pixel

For a loaded ant, it searches for the similar cell where it can drop the pixel. As discussed in the basic ant clustering model, in the AntClust algorithm, small lists of recently visited cells are also maintained for each ant. For dropping a pixel, the cells in the memory are considered and choose the most similar cell to drop the pixel. The drop probability is computed as

$$p_{drop}(p_i, c_k) = 1 - cos^2(\frac{\pi}{2} f(p_i, c_k)) \tag{10}$$

Ant System based Contour Clustering Model for Image Segmentation

The ant clustering algorithm is achieving significant results for image segmentation problems. However, the following characteristics show the inefficiency of the ant clustering.

All the image pixels have to be either picked or dropped at least once, which increases computation cost.

There is no optimal value to initialize the ant system parameters like the number of ants, maximum number of iterations, and thresholds employed in the similarity functions.

The Ant Clustering algorithm specifically converts 2D image pixels into 1D, which seems to be an additional step that could be avoided as the segmentation algorithm has to detect the suspicious the region in the image grid.

 https://doi.org/10.37896/pd91.4/91426

ISSN: 0369-8963

The proposed Ant System based Contour Clustering (ASCC) based image segmentation simulates an exciting behavior of real time ants. In real-time, once an ant finds the food source, and then the other ants from the same colony are started surrounding the food source as shown in Fig.3. This point motivates this research work to extract the boundary of the surrounding region as a contour of the mass region to be segmented.

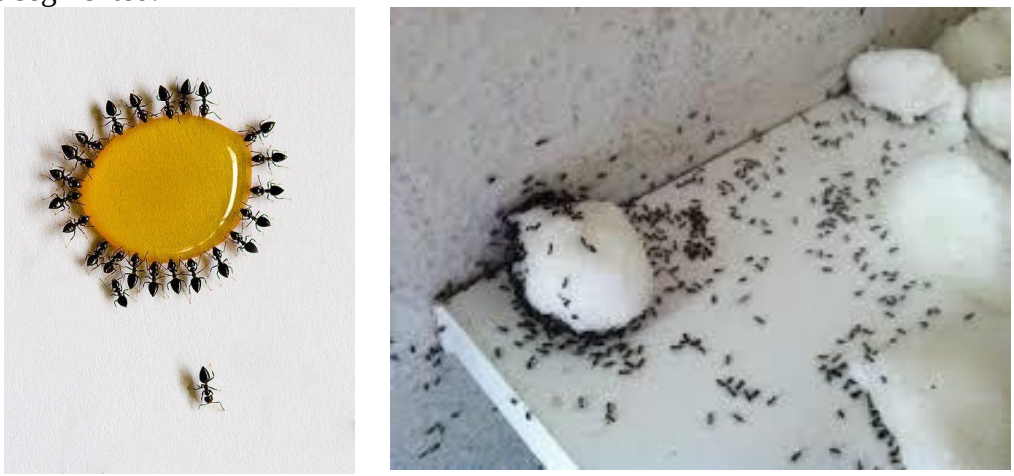

(a) (b)

Fig.3. Ants behaviour (a) Ants surrounds the food source (b) Dense ants over the food source

The proposed ASCC algorithm assumes that there is exactly only one abnormality region, which means that there are two kinds of tissues exist in the image; the background (normal) and the foreground (abnormal). ASCC algorithm, initially place one ant at the first & last row as well column of the image grid as shown in Fig.4., with the grid size as 10×10, and each 'A' represents an ant agent.

A	A	A	A	A	A	A	A	A	A
A									A
A									A
A									A
A									A
A									A
A									A
A									A
A									A
A	A	A	A	A	A	A	A	A	A

Fig.4. Sample image grid with initial ant position

Hence, for an image dimension $m \times n$, the ASCC algorithm initializes the number of ants (k) as

$$k = 2m + 2n - 4 \quad (11)$$

It is noted that most of the ant based algorithms initialize the number of ants with some real number at random. In ASCC, the numbers of ants are computed based on the image dimension, which resolves the problem of optimizing the 'number of ants' parameter. From the initialized ants, 5% of ants from each row & column are chosen for foraging and the rest of the ants are kept in the wait state. This is to avoid collision and to reduce the time complexity of the algorithm. The ants chosen for foraging are called as marker ants (M), and the rest of the ants are called as walker ants (W). Fig.5 illustrates a typical initialization of the image grid with a set of marker and walking ants. For the same image as

https://doi.org/10.37896/pd91.4/91426

ISSN: 0369-8963

shown in Fig.4 for the demonstration, one ant from each row & column is chosen as marker ant and rest of them are in idle state.

W	W	M_1	W	W	W	W	W	W	W
W									W
W									M_2
W									W
W									W
M_4									W
W									W
W									W
W									W
W	W	W	W	M_3	W	W	W	W	W

Fig.5. Sample image grid with Marker and Walker Ants position

The segmentation phase starts with the marker ants; they are allowed to search for a suspicious (abnormal) pixel in the image grid with a random walk. Initially, a marker ant is loaded with a pixel from its neighbor. The pixels' similarity with its neighbor is estimated as given in Equation (9), and the decision to drop the pixel is decided based on the drop probability as defined in Equation (10). If the drop probability is smaller than a random number, then the marker ant is allowed to search for the next pixel. Otherwise, the mean value of the surrounding neighbors is estimated and compared with a threshold value. For a pixel p, located at (x, y), the mean of its neighbor is computed as

$$\mu = \frac{1}{9}\sum_{i=x-1}^{x+1}\sum_{j=y-1}^{y+1} p(i,j) \tag{12}$$

If the mean value is greater than the threshold, then the pixel will be marked as a contour pixel, then the same procedure is repeated for the other ants in the marker set. If the mean value of the surround pixel is smaller than the threshold, then the marker ants drop the current pixel and choose another pixel from its neighbor.

$$contour\_pixel = \begin{cases} 1 & if\ \mu \geq threshold \\ 0 & Otherwise \end{cases} \tag{13}$$

For example, after several iterations, the marker ants could be placed as shown in Fig.6. When all the marker ants end up with the abnormal pixel, a convex hull is constructed with their current position, and the center of the hull is computed $(H_{x,y})$ as illustrated in Fig.7. The convex hull generated with the marker ants might generate a rough boundary over the mass region of the mammogram. The boundary constructed from the convex hull will be refined with the walker ants. At the second stage, the walker ants are resumed from the idle state and start moving towards the convex hull center $H_{x,y}$. This movement of walker ant is a directed one, as they are restricted to travel through straight line that is established between the current spatial location of the walker ant and the hull center.

 https://doi.org/10.37896/pd91.4/91426

ISSN: 0369-8963

W	W		W	W	W	W	W	W	W
W									W
W									
W				M_1					W
W							M_3		W
									W
W		M_4							W
W									W
W							M_2		W
W	W	W	W		W	W	W	W	W

Fig.6. A typical output of selected contour pixels from marker ants

W	W		W	W	W	W	W	W	W
W									W
W									
W				M_1					W
W							M_3		W
									W
W		M_4			**H**				W
W									W
W							M_2		W
W	W	W	W		W	W	W	W	W

Fig.7. A typical convex hull and its center

The straight line is computed using the basic Bresenham's line drawing algorithm. While walking along the straight line, the drop probability and the neighboring mean is estimated as similar to the procedure followed for the marker ants for every encountering pixel. The walk on the straight line is continued. They either found a contour pixel or they reached the hull center. Once all the walker ants have completed their walk, then the convex hull is reconstructed with all the ants' current spatial locations. And the contour of the convex hull would be the refined boundary that defines the abnormal region of the mammogram image. Fig. 8(a) depicts a typical path of a walker ant and their final position in Fig. 8(b). More than one walker ant might end up at the same pixel location; hence there is a chance for overlapping.

https://doi.org/10.37896/pd91.4/91426

ISSN: 0369-8963

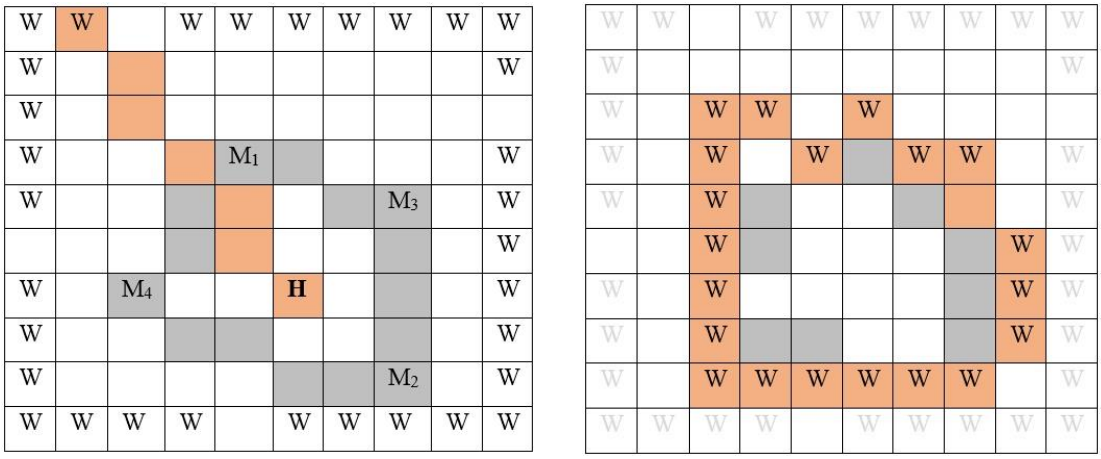

Fig.8. (a) A straight line path for a walker ant (b) refined contour with the location of all walker ants

The following pseudocode summarizes the Ant System based Contour Clustering (ASCC) algorithm based mammogram segmentation.

Algorithm – Ant System based Contour Clustering (ASCC)

Input – Digital Mammogram Image
Output – Segmented Mammogram Image
/* Ant Initialization */
Place each ant a_i at every border pixel p_i (surrounding the image)
Categorize the ants as Marker (M) and Walker (W) ants
For each marker ant
    Compute $f(p_i, c_k)$ and $p_{drop}(p_i, c_k)$
    Select a random number R between 0 and 1
    If $\left(R \leq p_{drop}(p_i, c_k))\right)$ then
        Move a_i to the next adjacent pixel p_i
    Else
        Find the mean (μ) of the neighbors,
        If $\mu >$ th
            $p_c \leftarrow (x, y)\ of\ p_i$, contour pixel
            Break;
        End If
    End If
End For
Construct the Convex Hull with the current positions of Marker Ants
Computer the Convex Hull center (H)
For each walker ant
    Draw a straight line from its current pixel position (p_i) to H
    /* straight line is drawn using Bresenham's line drawing algorithm */
    For each pixel in the straight line path
        Compute $f(p_i, c_k)$ and $p_{drop}(p_i, c_k)$
        Select a random number R between 0 and 1

 https://doi.org/10.37896/pd91.4/91426

ISSN: 0369-8963

If $\left(R \leq p_{drop}(p_i, c_k))\right)$ then
Move a_i to the next pixel in the path, p_i
Else
Find the mean (μ) of the neighbors,
If $\mu >$ th
$p_c \leftarrow (x, y)\ of\ p_i$, add the pixel to the contour
Break;
End If
End If
End For
End For
Refine the convex hull with the current positions of Walker Ants
Extract the segmented region surrounded by the contour pixel.

RESULTS

The segmentation performance of the proposed Ant System based Contour Clustering (ASCC) method is evaluated with the area, pixel and edge based metrics on the Mammographic Image Analysis Society (MIAS) Dataset. The Ant Colony Optimization (ACO) based segmentation [7, 8], Fuzzy C-means (FCM) clustering [16], Level Set (LS) segmentation [17], Active Contour (AC) based segmentation [18], Threshold based segmentation (TS) [19], and K-means clustering [24] are evaluated on the same dataset of the proposed ASCC algorithm and compared to know its state of art performance.

Experimental Data

The proposed segmentation algorithm is evaluated with the mammogram images received from the Mammographic Image Analysis Society (MIAS). This dataset consists of 312 mammograms acquired from 161 patients. For each of them, the left and right breasts are screened. This dataset is free to access, the digitized mammogram in this dataset has the following properties.

- The mammograms are captured in MLO view.
- All the images are captured with 200□m per pixel. The dimension is 1024 × 1024 pixels wide and height in the unit of pixels.
- The mammograms are gray-scaled images, each pixel has an 8-bit depth, means that their intensity value ranges between 0 and 255.
- Each mammogram is serially numbered, and provided with the information like the type of abnormality, spatial location & surrounding radius of the masses, and their respective class (benign / malignant).
- There were 146 symmetric and 15 asymmetric pairs of mammograms.

Evaluation Criteria

The segmentation performance of the proposed Ant System based Contour Clustering (ASCC) method is evaluated with the area, pixel and edge based metrics. These evaluation metrics are obtained for each of the recent segmentation techniques on the same dataset used by the proposed ASCC algorithm.

 https://doi.org/10.37896/pd91.4/91426

ISSN: 0369-8963

Area based metrics

The area-based methods generally overlap the segmented and the reference region and estimate the size of the common area between them. The Jaccard Index (JI), Relative Foreground Area Error (RAE), Goodness based on intra-region Uniformity (GU), and Goodness based on intra- region Contrast (GC) are the area based measures used in this research work.

Jaccard index [27] is a metric used to measure the overlap between the segmented region (S) and the ground truth region (R). It is computed as

$$JI = \frac{|S \cap R|}{|S \cup R|} \tag{14}$$

Sezgin and Sankur [28] proposed a Relative Foreground Area Error (RAE) to compare the shape and area between the reference and segmented regions. It is estimated as

$$RAE = \begin{cases} \frac{|R|-|S|}{|R|} & if\ |S| < |R| \\ \frac{|S|-|R|}{|R|} & if\ |S| \geq |R| \end{cases} \tag{15}$$

where $|R|$ and $|S|$ denotes the total number of pixels available in the reference and segmented regions respectively. A zero indicate the accurate segmentation, and the 1 denote the inexact segmentation.

Zhang [29] reported that the segmented region should have greater intra-region uniformity, which is based on variance of the pixels belonging to that region. A goodness measure can be used to estimate the intra-region uniformity. For a gray-level image $f(x, y)$, S_i be the ith segmented region, then the Gray-level Uniformity (GU) measure is computed as

$$GU = \sum_i \sum_{(x,y)\in S_i} \left[f(x,y) - \frac{1}{|S_i|} \sum_{(x,y)\in S_i} f(x,y) \right]^2 \tag{16}$$

Goodness based on inter-region contrast in [29] reported that the segmented regions should have greater contrast when compared to neighborhood regions. For a gray–level image, with the average gray-level for the object (mass) pixels f_M and f_B as the average backgroud gray-level, the Goodness based on inter-region Contrast (GC) is estimated as

$$GC = \frac{|f_M - f_B|}{f_M + f_B} \tag{17}$$

The greater GC value indicate better separation between regions.

Pixel based metrics

The pixel-based segmentation evaluation measures quantify the performance based on the number of correctly segmented and missegmented pixels from the background and foreground of the image. Segmentation Error (SE), Distance Error (DE), Overlay Index (OI), Precision, Recall, F-Measure, Specificity, and Balanced Accuracy are the pixel-based measures used in this research work.

Yasnoff et al. [30] proposed an area based metric, segmentation error SE, that indicate the proportion of misclassified pixels to the whole ROI. Segmentation Error (SE) is computed as

$$SE = 1 - \frac{|B_S \cap B_R| + |M_S \cap M_R|}{|B_S + M_R|} \tag{18}$$

Where B and M denotes the background and the mass pixels, subscript S and R represent the segmented and reference (ground truth) regions. The $|.|$ notation denote the cardinality of the pixel set. The lower the error indicates better segmentation performance. But, this measure fails when the actual mass region is very small, though the segmentation would not be able to locate any of the mass pixel.

 https://doi.org/10.37896/pd91.4/91426

ISSN: 0369-8963

Yasnoff et al. [30] proposed another metric, Distance Error (DE) which considers the spatial distance between the misclassified pixels and the actual location to overcome the issues of SE metric. Let M be the total number of missegmented pixels, for each of them, the spatial distance d_i between the ith mis-segmented pixel and the nearest pixel from the reference region is computed. This distance is squared and summed to compute the total error as follows:

$$D = \sum_{i=1}^{M} d_i^2 \tag{19}$$

This metric is further normalized by with the total number of pixels (n) in the reference region, to make the measure size independent.

$$DE = 100 \times \frac{\sqrt{D}}{n} \tag{20}$$

Sampaio et al. [31] presented an Overlay Index (OI) measure to analyze the segmentation performance by estimating the mean ratio between area of the detected mass and ground truth area. It is expected to have 1 for this index to indicate accurate segmentation. If the located area is greater than the index value will be greater than 1, or else it will be smaller than 1. The OI is defined as

$$OI = \frac{\sum_{i=1}^{n} \frac{D_i}{S_i}}{n} \tag{21}$$

where D_i is the number of pixels in the detected mass region, S_i is the number of pixels from the ground truth mass region, and n is the total number of mammogram images examined.

Rosa et al. [32] prepared a confusion matrix to evaluate the segmentation with precision, recall and F-measures. The respective measures are computed as follows:

$$Precision = \frac{|M_S \cap M_R|}{|M_S \cap M_R| + |M_S \cap B_R|} \tag{22}$$

$$Recall/Sensitivity = \frac{|M_S \cap M_R|}{|M_S \cap M_R| + |B_S \cap M_G|} \tag{23}$$

$$F = 2 \times \frac{Precision \times Recall}{Precision + Recall} \tag{24}$$

In additions to that, the following metric to evaluate the specificity of the segmentation.

$$Specificity = \frac{|M_S \cap M_R|}{|B_S \cap M_R| + |B_S \cap B_G|} \tag{25}$$

Edge based metrics

The edge-based segmentation evaluation measures compare the goodness of the boundaries between the segmented and the reference regions. The Hausdorff Distance (H), Over-segmented Pixel Rate (ODI), Under-Segmented Pixel Rate (UDI), Region Non-Uniformity (NU), Edge Mismatch (EMM), and Figure of Merit (FOM) are the edge-based metrics, computed to analyze the segmentation performance. Edge based measures are used to evaluate the boundary between the reference and segmented region. Initially the edge pixels of both the regions are stored in two sets $A = \{a_1, a_2, \dots, a_n\}$ and $B = \{b_1, b_2, \dots, b_3\}$, where a_i and b_i are the edge points. The minimum distance from the edge pixels of A set to B is computed as

$$d(a_i, B) = \min_j \left\| b_j - a_i \right\| \tag{26}$$

The distance between two edges could be measured with Hausdorff Distance (H) measure [33], defined as

$$H(A, B) = max\left(\max_i \{ d(a_i, B) \}, \max_j \{ d(b_j, A) \} \right) \tag{27}$$

The Hausdorff distance measure quantifies the common edge dissimilarity between two boundaries. Odet et al. [34] proposed two other metrics to estimate the under-segmented (UDI) and over-segmented

 https://doi.org/10.37896/pd91.4/91426

ISSN: 0369-8963

(ODI) pixel rate, defined as

$$ODI = \frac{1}{N_O}\sum_{i=0}^{N_O}\left(\frac{d_O(i)}{d_{TH}}\right)^p \quad (28)$$

$$UDI = \frac{1}{N_U}\sum_{i=1}^{N_U}\left(\frac{d_U(i)}{d_{TH}}\right)^p \quad (29)$$

Where N_O and N_U are the edge pixel count at over- and under-segmented regions, d_O and d_U are the distances of over- and under-segmented pixels, dTH is the upper bound distance, and p is the the scale factor for distances lower than upper bound.

The Non-Uniformity (NU) metric is used to quantify the segmentation performance within the range between 0 and 1. The measure is defined from [29] and is given as

$$NU = \frac{|M_S|.\sigma_M^2}{|M_S+B_S|.\sigma^2} \quad (30)$$

Where M_S and B_S are the total number of mass and background pixels available in the segmented region, σ_M^2 and σ^2 are the pixel intensity variation in the mass and for the entire region respectively

Sezgin and Sankur [28] proposed a novel measure Edge Mismatch (EM) metric to estimate the edge dissimilarity. It is defined as

$$EM = 1 - \frac{|A\cap B|}{|A\cap B| + \alpha\sum_{k\in|A-B|}\delta_k + \beta\sum_{k\in|B-A|}\delta_k} \quad (31)$$

$$\delta_k = \begin{cases} |d_k| & if\ |d_k| < maxdist \\ d_{max} & otherwise \end{cases}$$

Where $|A \cap B|$ denotes the total number of common edge pixels exist in both reference and segmented region, $|A - B|$ and $|B - A|$ denotes the number of edge pixels in one region and not in the other, α and β are the penalties associated with the excess segmented and reference pixels. Sezgin and Sankur [28] suggested the following values for the respective factors, where N is the image dimension.

$$maxdist = 0.025N, d_{max} = 0.1N, \alpha = 10/N, \beta = 2$$

The margin of the segmented region could be compared with the boundary of the reference region using a distance measure called Figure of Merit (FOM) as defined in [29] is given below.

$$FOM = \frac{1}{n}\sum_{i=1}^{n}\frac{1}{1+p\times d^2(i)} \quad (32)$$

where n denotes the number of edge pixels, $n = \max(n_S, n_R)$, from the segmented or the reference region, $d(i)$ represent the distance between the estimated and actual edge pixel, and p is the scaling factor. Zhang [29] discussed that this metric is insensitive to noises and false positives.

Evaluated Experimental Results

On the Mammographic Image Analysis Society (MIAS) Dataset, the proposed Ant System based Contour Clustering (ASCC) method's segmentation performance is tested using area, pixel, and edge based metrics. On the same dataset as the proposed ASCC algorithm, the Ant Colony Optimization (ACO) based segmentation [7, 8], Fuzzy C-means (FCM) clustering [16], Levet Set (LS) segmentation [17], Active Contour (AC) based segmentation [18], Threshold based segmentation (TS) [19], and K-means clustering [24] are evaluated and compared. To know the overlaps between the segmented and the reference region and to estimate the size of the common area between them, the area based metrics such as Jaccard Index (JI), Relative Foreground Area Error (RAE), Goodness based on intra-region Uniformity (GU), and Goodness based on intra- region Contrast (GC) are evaluated for the proposed ASCC algorithm along with other existing algorithms. Further, to quantify the segmentation performance based on the number of correctly segmented and missegmented pixels from the background and foreground of the image, the pixel based metrics such as Segmentation Error (SE),

 https://doi.org/10.37896/pd91.4/91426

ISSN: 0369-8963

Distance Error (DE), Overlay Index (OI), Precision, Recall, F-Measure, and Specificity are evaluated on the proposed and existing algorithms. Furthermore, to compare the goodness of the boundaries between the segmented and the reference regions, the proposed and existing algorithms are evaluated with edge based metrics such as Hausdorff Distance (H), Over-segmented Pixel Rate (ODI), Under-Segmented Pixel Rate (UDI), Region Non-Uniformity (NU), Edge Mismatch (EMM), and Figure of Merit (FOM).

The following Table 1, quantifies the performance of segmentation with area based evaluation measures. The segmentation performance comparison of the proposed ASCC algorithm with the other existing algorithms with respect to the area based metrics is depicted graphically in the Fig.9. The proposed ASCC algorithm outperforms the other segmentation methods with better quantitative rates for all the areas based measures compared to other algorithms mentioned.

Table 1. Segmentation Performance with area based metrics

Methods	JI	GC	RAE	GU
ASCC	**0.6247**	**0.6659**	**0.1668**	**0.2557**
ACO	0.6237	0.6583	0.2592	0.3128
FCM	0.6224	0.6015	0.3364	0.3586
LS	0.6223	0.5857	0.3814	0.3689
AC	0.5484	0.5746	0.3841	0.3712
TS	0.5374	0.5669	0.4222	0.3859
k-means	0.4784	0.5648	0.4366	0.3994

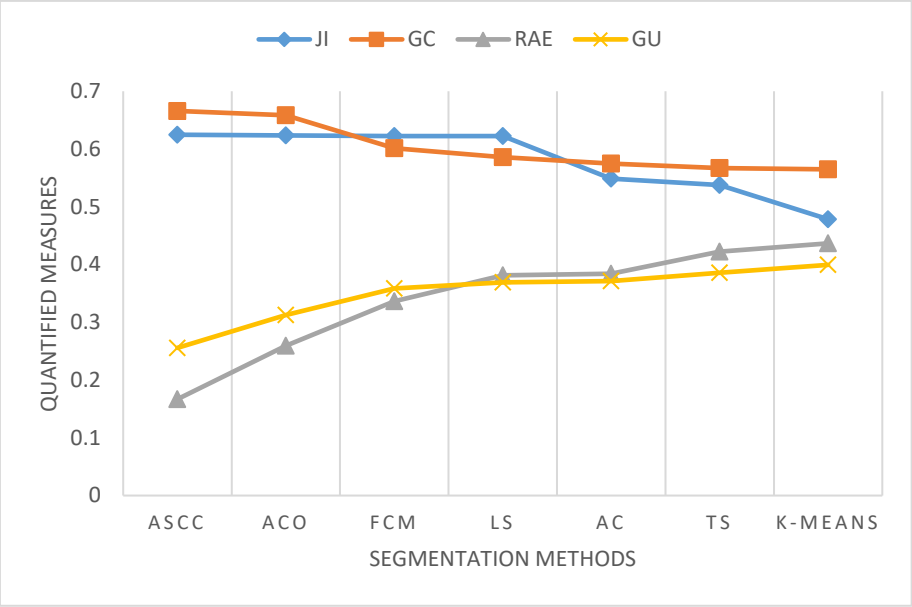

Fig.9. Performance comparison of segmentation methods with area based metrics

The following Table 2, quantifies the performance of segmentation with area based evaluation measures.

Table 2. Segmentation Performance with Pixel based metrics

Methods	SE	DE	OI	Precision	Recall	F	Specificity
ASCC	**9.5149**	**0.2298**	**0.7470**	**93.6716**	**90.9009**	**0.8377**	**89.6316**
ACO	16.6124	0.3126	0.7155	86.7918	89.0544	0.7721	86.6246
FCM	18.2309	0.3267	0.7051	81.3138	83.8751	0.7526	86.1937

https://doi.org/10.37896/pd91.4/91426

ISSN: 0369-8963

LS	19.6669	0.3768	0.6393	78.6966	79.7748	0.4090	85.6961
AC	26.0971	0.3970	0.5459	73.2327	71.9527	0.3382	84.6260
TS	29.3270	0.4150	0.4983	70.4181	69.0309	0.3302	82.9232
k-means	32.5101	0.4245	0.4800	69.3858	68.7429	0.2955	81.5152

The segmentation performance comparison of the proposed ASCC algorithm with the other existing algorithms with respect to the pixel based metrics is depicted graphically in the following Fig.10. The proposed ASCC algorithm outperforms the other segmentation methods with better quantitative rates for all the pixel based measures compared to other algorithms mentioned.

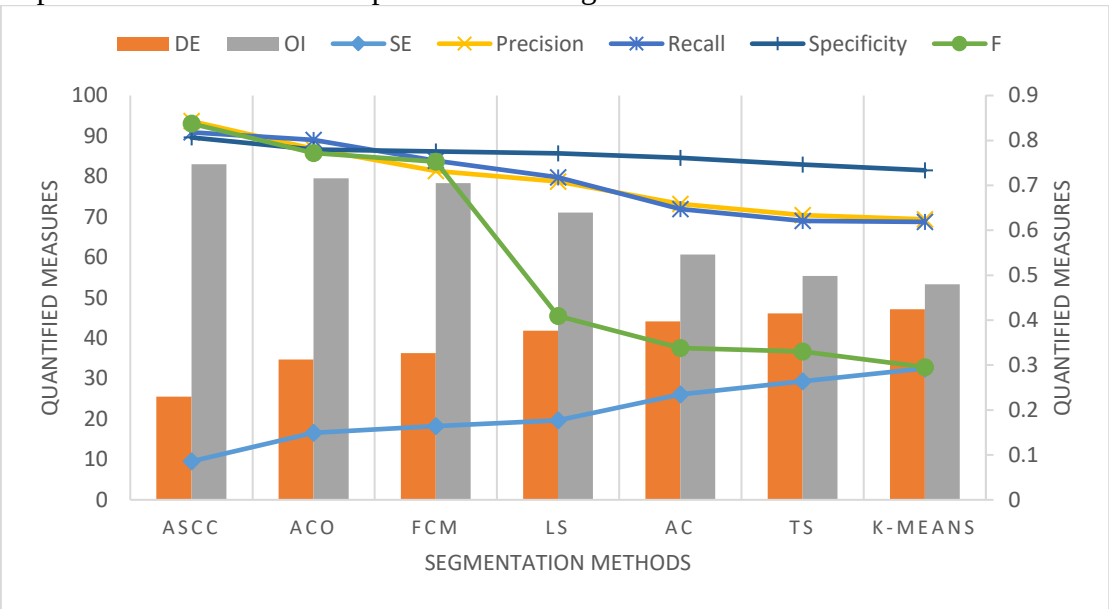

Fig.10. Performance comparison of segmentation methods with pixel based metrics

The following Table 3, quantifies the performance of segmentation with edge based evaluation measures.

Table 3. Segmentation Performance with Edge based metrics

Methods	H	ODI	UDI	NU	EM	FOM
ASCC	**35.5640**	**0.0043**	**0.0026**	**0.0234**	**0.1864**	**0.8549**
ACO	75.8811	0.0104	0.0357	0.0413	0.2020	0.7933
FCM	94.0456	0.0376	0.0364	0.0601	0.2181	0.7594
LS	130.0218	0.0425	0.0685	0.0752	0.2831	0.7314
AC	165.7160	0.0455	0.0742	0.0804	0.3434	0.5122
TS	166.3824	0.0623	0.1163	0.0839	0.3618	0.2904
k-means	197.1012	0.0747	0.1747	0.0898	0.3792	0.2231

The segmentation performance comparison of the proposed ASCC algorithm with the other existing algorithms with respect to the edge based metrics is depicted graphically in the following Fig.11. The proposed ASCC algorithm outperforms the other segmentation methods with better quantitative rates for all the edge based measures compared to other algorithms mentioned.

https://doi.org/10.37896/pd91.4/91426

ISSN: 0369-8963

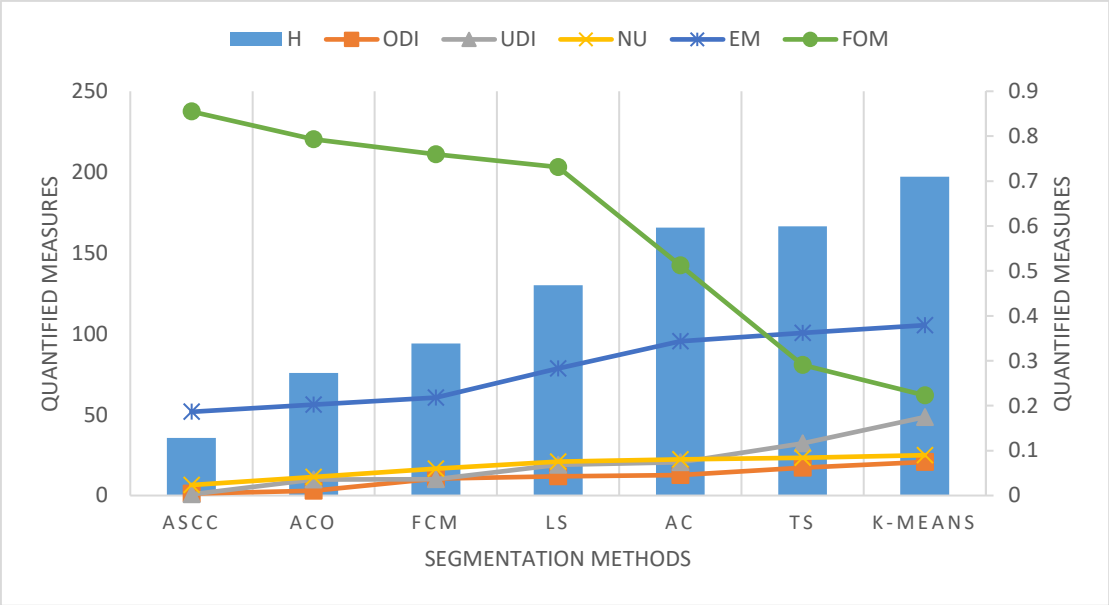

Fig.11. Performance comparison of segmentation methods with edge based metrics

The qualitative typical segmentation outputs for the Ant Clustering algorithm are shown in the Fig.12. When it comes to image segmentation, the ant clustering technique delivers impressive results. The ant clustering, on the other hand, has a number of flaws. An ant system's parameters such as number of ants or iterations and thresholds used in the similarity functions have no optimum value. While the Ant Clustering technique uses a 2D image pixel grid to identify suspicious regions, it appears to be an unnecessary step because the segmentation algorithm already has to identify these regions in the image grid.

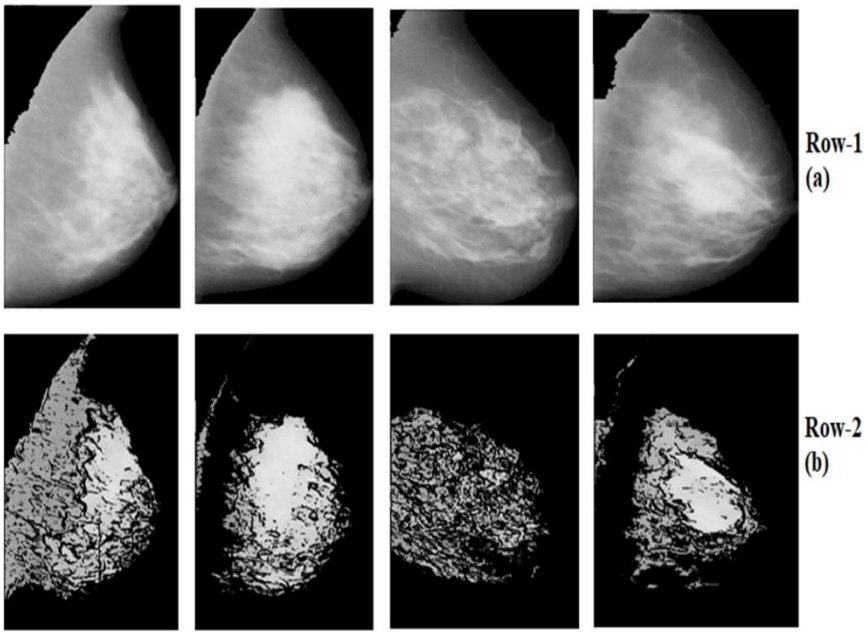

Fig.12. Ant Clustering Algorithm (a) Row-1: Original Mammogram Images (b) Row-2: Segmented Output Images

https://doi.org/10.37896/pd91.4/91426

ISSN: 0369-8963

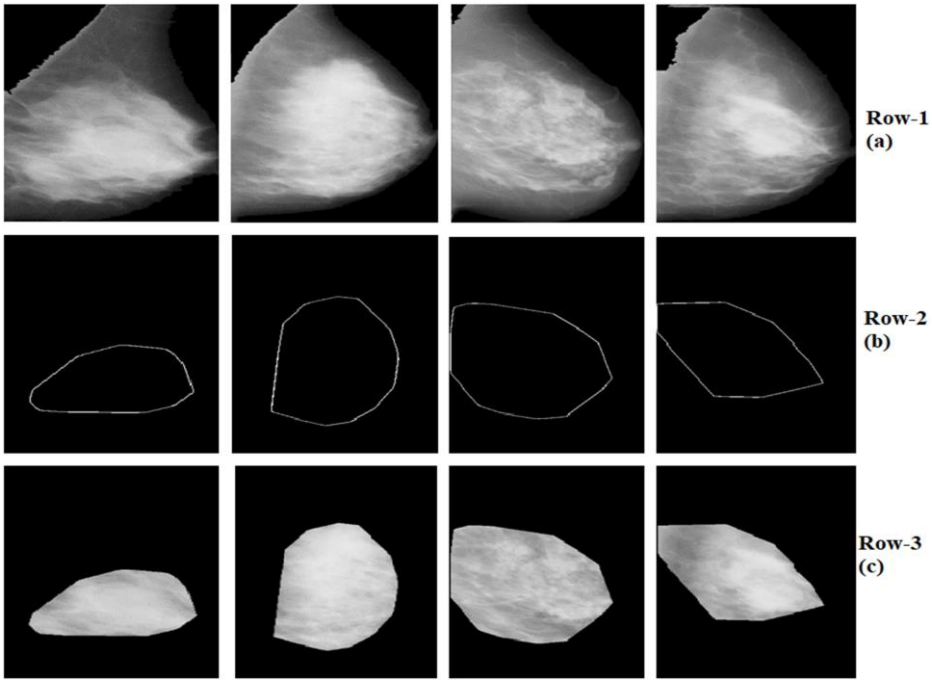

Fig.13. Ant System based Contour Clustering Algorithm (a) Row-1: Original Mammogram Images (b) Row-2: Contour of the Suspicious Region (c) Row-3: Segmented Output Images

The qualitative typical segmentation outputs for the Ant Clustering algorithm are shown in the Fig.13. When it comes to the proposed ASCC algorithm, only the drop probability is estimated for the pixels, the pick is based on the neighboring mean and also the number ant agent is estimated rather than initializing with the random number.

DISCUSSION

The segmentation performance of the proposed Ant System based Contour Clustering (ASCC) method is evaluated with the area, pixel and edge based metrics on the Mammographic Image Analysis Society (MIAS) Dataset. Table 1, shows the area based metrics with Jaccard Index (JI) of 62.47%, Goodness based on intra-region Contrast (GC) of 66.59%, Relative Foreground Area Error (RAE) of 16.68% and Goodness based on intra-region Uniformity (GU) of 25.57%. All these edge based metrics showing superiority of the proposed ASCC algorithm compared to other existing methods. Table 2 shows the evaluation of the pixel based metrics for the proposed ASCC algorithm with Segmentation Error (SE) of 9.51%, Distance Error (DE) of 0.22%, Overlay Index (OI) of 74.70%, Precision of 93.67%, Recall of 90.90%, F-Measure of 83.77% and Specificity of 89.63%. These entire pixel-based metrics showing superiority of the proposed ASCC algorithm compared to other existing methods. Table 3 shows the performance of segmentation of the proposed ASCC method with the help of edge based measures. For proposed algorithm, the edge based metrics such as Hausdorff Distance (H) value of 35.56%, Over- segmented Pixel Rate (ODI) of 0.43%, Under-Segmented Pixel Rate (UDI) of 0.26%, Region Non-Uniformity (NU) of 2.34%, and Edge Mismatch (EMM) of 18.64% and Figure of Merit (FOM) of 85.49% are obtained. These entire edge based metrics show the superiority of the proposed ASCC algorithm compared to other existing methods.

Existing approaches must process every pixel of an image, which is expensive. Ant Colony Optimization can detect microcalcifications in digital mammograms. Ant clustering achieves remarkable results for image segmentation. Picking or dropping every pixel increases computing time.

 https://doi.org/10.37896/pd91.4/91426

ISSN: 0369-8963

There is no best value for initializing ant system parameters such as number of ants, maximum iterations, and similarity function thresholds. The Ant Clustering technique, which converts 2-D pixels to 1-D, seems superfluous for image segmentation. For this study, the surrounding region's boundary will be employed as a contour to segment the mass region to be studied. The advantages of the proposed ASCC based image segmentation are: the number ant agent is estimated rather than initializing with the random number; the termination condition for each ant is to end up with a contour pixel rather than fixing it with maximum number of iterations; only the drop probability is estimated for the pixels, the pick is based on the neighboring mean. Definitely the ASCC algorithm doesn't evaluate each and every pixel in the image, and moreover the pixels are retained at their original position rather than moving them to form the clusters.

CONCLUSIONS

Detecting the abnormalities in digital mammogram is the key preprocessing technique for the accurate diagnosis. A novel Ant System based segmentation is proposed in this paper for efficient mammogram segmentation. The proposed Ant System based Contour Clustering (ASCC) is a hybridization of clustering and contour based segmentation approaches. Here the Ant System parameters like number of ants and the maximum number of iterations are computed rather than initializing them. And, the time complexity of the clustering process is reduced by investigating limited number of pixels rather than testing the entire pixels in the image grid as conventional clustering methods do. The proposed ASCC method does not require any heap memory storage for the ants to remember their recently visited locations. With all these merits, the segmentation performance of the proposed ASCC is evaluated with the mammogram images received from MIAS database. The performance metrics and the comparative results shows that the proposed ASCC based segmentation is more efficient than the other recently reported methods.

Funding
None

Conflict of interest
This work is not related with any situations that could be seen as a conflict of interest.

Ethical approval
In this research, not one of the writers' reports seeing any research that included either human or animal participants in the trials.

REFERENCES

1. D. Cascio et al., Mammogram Segmentation by Contour Searching and Mass Lesions Classification With Neural Network, IEEE Transactions on Nuclear Science 53(5)(2006), 2827-2833.
2. F. Bray, J. Ferlay, I. Soerjomataram, R. Siegel, L. Torre and A. Jemal, Global cancer statistics 2018: Globocan estimates of incidence and mortality worldwide for 36 cancers in 185 countries, CA Cancer J Clin 1 (2018), 1-30.
3. D. Maggio, Cosimo, State of the art of current modalities for the diagnosis of breast lesions, European Journal of Nuclear Medicine & Molecular Imaging 30(1) (2004), S56– S69.
4. Dixon, A.M. Diagnostic Breast Imaging: Mammography, Sonography, Magnetic Resonance Imaging, and Interventional Procedures, Ultrasound: Journal of the British Medical Ultrasound Society, 22(3) (2014), 182-183.

 https://doi.org/10.37896/pd91.4/91426

ISSN: 0369-8963

5. Kanadam, K.P., and Chereddy, S.R., Mammogram classification using sparse-ROI: A novel representation to arbitrary shaped masses, Expert Systems with Applications 57(2016), 204-213.
6. Birdwell, R.L., Ikeda, D.M., O'Shaughnessy, K.F., and Sickles, E.A., Mammographic characteristics of 115 missed cancers later detected with screening mammography and the potential utility of computer-aided detection, Radiology 219(1) (2001), 192-202.
7. Ouadfel, S., Batouche, M., and Garbay, C., Ant colony system for image segmentation using Markov random field, In Proceedings of the International Workshop on Ant Algorithms, September 12-14; Brussels, Belgium (2002), 294-295.
8. Han, Y., and Shi, P., An improved ant colony algorithm for fuzzy clustering in image segmentation, Neurocomputing 70(4-6) (2007), 665-671.
9. Abdullah, H.S., and Jasim, A.H., Improved Ant Colony Optimization for Document Image Segmentation, International Journal of Computer Science and Information Security 14(11) (2016), 775-785.
10. Khorram, B., and Yazdi, M., A new optimized thresholding method using ant colony algorithm for MR brain image segmentation, Journal of Digital Imaging 32(1) (2019), 162-174.
11. Estevez, L., Kehtarnavaz, N., and Wendt, R., Interactive selective and adaptive clustering for detection of microcalcifications in mammograms, Digital Signal Processing 6 (1996), 224-232.
12. Riyahi-Alam, N., Ahmadian, A., Tehrani, J. N., Guiti, M., Oghabian, M. A., & Deldari, A., Segmentation of suspicious clustered microcalcifications on digital mammograms: using fuzzy logic and wavelet coefficients, In IEEE Proceedings 7th International Conference on Signal Processing, 31(3) (2004), 2226-2228.
13. Santoro, M., Prevete, R., Cavallo, L., and Catanzariti, E., (2005). Mass detection in mammograms using Gabor filters and fuzzy clustering. In Proceedings of the International Workshop on Fuzzy Logic and Applications, September 15-17; Crema, Italy, (2005), 334-343.
14. Bhattacharya, M., and Das, A., Fuzzy logic based segmentation of microcalcification in breast using digital mammograms considering multiresolution, In Proceedings of the International Machine Vision and Image Processing, September 5-7; Kildare, Ireland, (2007), 98-105.
15. Boss, R.S.C., Thangavel, K., and Daniel, D.A., Mammogram image segmentation using fuzzy clustering, In IEEE Proceedings of the International Conference on Pattern Recognition, Informatics and Medical Engineering, March 21-23; Salem, India, (2012), 290-295.
16. Chowdhary, C.L., and Acharjya, D.P., Segmentation of mammograms using a novel intuitionistic possibilistic fuzzy c-mean clustering algorithm. In Nature Inspired Computing, Singapore, (2018), 75-82.
17. Rouhi, R., and Jafari, M., Classification of benign and malignant breast tumors based on hybrid level set segmentation, Expert systems with Applications, 46 (2016), 45-59.
18. Duarte, M.A., Alvarenga, A.V., Azevedo, C.M., Calas, M.J.G., Infantosi, A.F., and Pereira, W.C., Evaluating geodesic active contours in microcalcifications segmentation on mammograms, Computer Methods and Programs in Biomedicine 122(3) (2015), 304- 315.
19. De Nazaré Silva, J., de Carvalho Filho, A.O., Silva, A.C., De Paiva, A.C., and Gattass, M., Automatic detection of masses in mammograms using quality threshold clustering correlogram function and SVM, Journal of Digital Imaging 28(3) (2015), 323-337.
20. Liu, X., Mei, M., Liu, J., and Hu, W., Microcalcification detection in full-field digital mammograms with PFCM clustering and weighted SVM-based method, EURASIP Journal on Advances in Signal Processing (1)2015, 1-13.
21. Sandhya, G., Gowda, M. S., Swamy, L. N., Raju, G. T., and Vasumathi, D., Automated detection of cancer tissues in mammograms using advanced K-Means clustering with homomorphic filtering, In Proceedings of the International conference on Circuits, Controls and Communications, December 27-28, Bengaluru, India. (2013), 1-4.

 https://doi.org/10.37896/pd91.4/91426

ISSN: 0369-8963

22. Elmoufidi, A., El Fahssi, K., Jai-Andaloussi, S., Madrane, N., and Sekkaki, A., Detection of regions of interest's in mammograms by using local binary pattern, dynamic k-means algorithm and gray level co-occurrence matrix, In IEEE Proceedings of the International Conference on Next Generation Networks and Services, May 28-30; Casablanca, Morocco, (2014),118-123.
23. Wan, K., and Zunaidi, I., An Efficient Data Mining Approaches for Breast Cancer Detection and Segmentation in Mammogram, Journal of Advanced Research in Dynamical and Control Systems, 9(3) (2017),185-194.
24. Moftah, H.M., Azar, A.T., Al-Shammari, E.T., Ghali, N.I., Hassanien, A.E., and Shoman, M., Adaptive k-means clustering algorithm for MR breast image segmentation, Neural Computing and Applications, 24(7-8) (2014), 1917-1928.
25. Deneubourg, J.L., Goss, S., Franks, N., Sendova-Franks, A., Detrain, C., and Chrétien, L., The dynamics of collective sorting robot-like ants and ant-like robots, In Proceedings of the 1st International Conference on simulation of adaptive behavior on From animals to animats, February; Paris, France, (1991), 356-363.
26. Lumer, E.D., and Faieta, B., Diversity and adaptation in populations of clustering ants, In Proceedings of the third international conference on Simulation of adaptive behavior: from animals to animats 3, August 8-12; Brighton, England, (1994), 501-508.
27. Jaccard, P., Nouvelles recherches sur la distribution florale, Bulletin Société Vaudoise des Sciences Naturelles 44 (1908), 223-270
28. Sezgin, M., and Sankur, B., Survey over image thresholding techniques and quantitative performance evaluation, Journal of Electronic imaging 13(1) (2004), 146-165.
29. Zhang, Y.J., A survey on evaluation methods for image segmentation, Pattern Recognition, 29(8) (1996), 1335-1346.
30. Yasnoff, W.A., Mui, J.K., and Bacus, J.W., Error measures for scene segmentation, Pattern Recognition, 9(4) (1977), 217-231.
31. Sampaio, W.B., Diniz, E.M., Silva, A.C., De Paiva, A.C., and Gattass, M., Detection of masses in mammogram images using CNN, geostatistic functions and SVM, Computers in Biology and Medicine, 41(8) (2011), 653-664.
32. Rosa, B., Mozer, P., and Szewczyk, J., An algorithm for calculi segmentation on ureteroscopic images, International Journal of Computer Assisted Radiology and Surgery, 6(2) (2011), 237-246.
33. Chalana, V., and Kim, Y., A methodology for evaluation of boundary detection algorithms on medical images, IEEE Transactions on Medical Imaging, 16(5) (1997), 642-652.
34. Odet, C., Belaroussi, B., & Benoit-Cattin, H., Scalable discrepancy measures for segmentation evaluation, In Proceedings of the International Conference on Image Processing, September 22-25; Rochester, USA, (2002), 1-1

 https://doi.org/10.37896/pd91.4/91426